UDK 669.715:669.721.5:620.193
Original scientific article/Izvirni znanstveni članek

ISSN 1580-2949
MTAEC9, 47(3)363(2013)

WELDED ALUMINIUM AND MAGNESIUM ALLOYS – CORROSION AND MECHANICAL PROPERTIES FOR REFRIGERATION COMPRESSORS IN COMPARISON WITH DEEP-DRAWING STEEL

VARJENE ALUMINIJEVE IN MAGNEZIJEVE ZLITINE – KOROZIJSKE IN MEHANSKE LASTNOSTI ZA KOMPRESORJE HLADILNIKOV V PRIMERJAVI Z JEKLOM ZA GLOBOKO VLEČENJE

Klaus Günther Kerschbaumer, Rudolf Vallant, Norbert Enzinger, Christof Sommitsch

Institute for Materials Science and Welding, Kopernikusgasse 24, 8010 Graz, Austria
rudolf.vallant@tugraz.at

Prejem rokopisa – received: 2012-10-03; sprejem za objavo – accepted for publication: 2012-11-12

Increasing the energy efficiency of household refrigeration appliances as a result of legal requirements is more and more important (2010/30/EUEG2010 Directive). This means that the equipment with the energy efficiency lower than D can no longer find its place in the European trading. In this investigation aluminium alloys (AW5083-O, AW6181-T4) and a magnesium alloy (AZ31) were selected via a material selection. They are compared to the currently used deep-drawing steels (DD11, DD13) with respect to the corrosion and strength properties of similar overlap-welded joints.
To verify the corrosion properties the neutral salt spray test (NSS) and the fruit acid spray test were performed with an overall test duration of 480 h. The type of corrosion, its influence on the corrosion rate and the strength of the welded joints were evaluated. Magnesium shows a very high corrosion and therefore cannot be used uncoated, like deep-drawing steel. The aluminium alloys show only slight selective corrosion phenomena and are, from the welding and corrosion point of view, an attractive alternative to steel. Due to a higher thermal conductivity of aluminium, in comparison with steel, a higher energy efficiency of the cooling compressor is expected.

Keywords: MIG/CMT-P welding, aluminium, magnesium, corrosion, deep-drawing steel, fruit acid, neutral salt spray test, tensile test, AW5083-O, AW6181-T4, AZ31, DD11, DD13, DIN 8985, DIN ISO 6227

Vedno bolj postaja pomembno povečanje energijske učinkovitosti gospodinjskih hladilnih naprav kot posledica legalnih zahtev (2010/30/EUEG2010 Directive). To pomeni, da oprema z energijsko učinkovitostjo, manjšo od D nima več mesta v evropski trgovini. V tej raziskavi sta bili pri izbiri materiala izbrani aluminijevi zlitini (AW5083-O, AW6181-T4) in magnezijeva zlitina (AZ31). Primerjane so s sedaj uporabljanima jekloma za globoko vlečenje (DD11, DD13) glede na korozijo in trdnostne lastnosti podobnih zvarov s prekrivanjem.
Za preverjanje korozijskih lastnosti sta bila izvršena preizkusa v nevtralni slani komori (NSS) in preizkus s škropljenjem sadne kisline v povprečnem trajanju 480 h. Na zvarjenih spojih je bila ocenjena vrsta korozije, vpliv na hitrost korozije in na trdnost zvarjenih spojev. Magnezij izkazuje veliko korozivnost in ga zato ni mogoče uporabljati brez površinske zaščite tako kot jeklo za globoki vlek. Aluminijevi zlitini izkazujeta samo rahle selektivne korozijske pojave in sta s stališča varjenja in korozije zanimivi kot alternativa za jeklo. Zaradi večje toplotne prevodnosti aluminija v primerjavi z jeklom se pričakuje tudi večja energijska učinkovitost kompresorja za hlajenje.

Ključne besede: MIG/CMT-P-varjenje, aluminij, magnezij, korozija, jeklo za globoki vlek, sadna kislina, nevtralni preizkus škropljenja s slanico, natezni preizkus, AW5083-O, AW6181-T4, AZ31, DD11, DD13, DIN 8985, DIN ISO 6227

1 INTRODUCTION

The main focus of the technological development of household cooling compressors is on an "energy-efficiency improvement" stimulated by the increased competition, cost pressures and a stricter EU legislation[1,2] for cooling compressors. Furthermore, the noise reduction in service and an improvement of the corrosion properties are important aims for a long-term system improvement of household cooling compressors. These future requirements can be met, in part, by finding a new, innovative housing material.

Currently, the steel materials DD11 and DD13 are used for deep-drawn, almost spherical housings.[3] The main problem is, however, that the material corrosion resistance in the above mentioned application is not satisfactory. Preliminary studies have shown that aluminum and magnesium alloys have a potential to replace the steel materials. For a material-selection process, according to Reuter[4], the following housing requirements have been defined:

- the minimum static strength of 85 MPa for the maximum internal pressure of 40 bar
- MIG or equivalent weldability
- the materials should be industrially formable (cold or hot forming)
- hermetic-gas proofness

The Al-alloys AW5083-O (annealed) and AW6181-T4 (naturally aged) and the magnesium alloy AZ31 were selected as suitable candidates for further investigations.

Corrosion investigations of these base materials and their similar welded joints in the neutral salt spray (NSS) and fruit acid spray tests (FS) have been performed.

2 EXPERIMENTAL WORK

2.1 Base materials and weld filler metals

MIG pulsed-arc welding was used for the annealed, AlMgMn, wrought alloy AW5083-0 and the naturally aged, AlMgSi, wrought alloy AW6181-T4. For the deep-drawing steels DD11 and DD13, MAG pulsed-arc welding was applied. The CMT+P welding procedure was applied for magnesium AZ31. The sheet thickness of the materials was 3 mm, except for the 2.5 mm AW6181-T4.

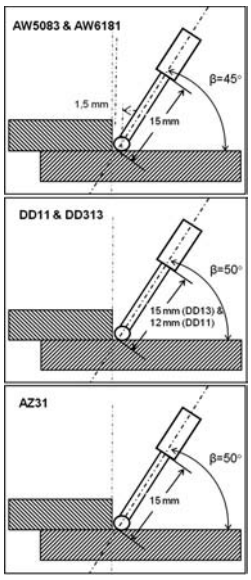

Figure 1: Welding-torch positions for similar overlap welded joints
Slika 1: Pozicija varilnika pri enako debelih prekrivnih varjenih spojih

The filler metals were selected according to the recommendations of DVS 0913[5] and Davis.[6] The AlMg5 filler was selected for AW5083-O, and AlSi5 for AW6181-T4. Considering the Böhler Welding Guide for DD11 and DD13, the G3Si1 (EMK6) filler was used[7]. For the AZ31 sheet, Kammer[8] recommends AZ61. AM50[9] was used as it easily meets the strength requirements of 85 MPa.

It is notable that the AlSi5 filler metal has only about 50 % of the strength of the AW6181-T4 sheet. Nevertheless, it was used as the hot-cracking susceptibility of 6000 alloys can be significantly reduced according to Davis.[6] The 440 MPa yield strength of the G3Si1 weld metal is much higher than the 170 MPa yield strength of deep-drawing steels, as there is no even matching filler available. The chemical compositions and mechanical properties of the examined sheet alloys and filler metals are summarized in **Table 1**.[3,7,9–12]

2.2 Experimental set-up and investigations

2.2.1 Welding experiments

In **Figure 1** the joint geometry and welding torch position are shown schematically for different material combinations. The top and bottom sheets were positioned with an overlap of 20 mm and clamped on the welding table. The welding experiments were carried out with a Fronius TPS4000+CMT welding machine. The torch was conducted with an ABB robot IRB140. The torch angle β varied between 45° and 50° depending on the material combinations. The contact tip distance

Table 1: Chemical analyses and mechanical properties of sheet alloys (GW) and weld-filler metals (FM)
Tabela 1: Kemijska analiza in mehanske lastnosti pločevin (GW) ter varilnega dodajnega materiala (FM)

material BM / FM element	AW5083-O (BM)[10]	AlMg5 (FM) [11]	6181-T4 (BM) [10]	AlSi5 (FM) [11]	DD11 (BM) [3]	DD13 (BM) [3]	EMK 6 (FM) [7]	AZ31 (BM) [12]	AM50A (FM) [9]
Si	0.4	<0.25	0.7–1.1	4.5–6.0			0.9		≤0.1
Fe	0.4	<0.4	0.15–0.5	<0.6	balance	balance	balance		≤0.008
Cu	0.1	<0.1	0.25	<0.3					≤0.01
Mn	0.4–1.0	0.05–0.2	0.4	<0.15	≤0.6	≤0.40	1.49	≤0.2	0.26–0.60
Mg	4.0–4.9	4.5–5.5	0.6–1.0	<0.2				balance	balance
Cr	0.05–0.25	0.05–0.2	0.15	-					
Zn	0.25	<0.1	0.3	<0.1				1.0	≤0.22
Ti	0.15	0.06–0.2	0.15	<0.15					
Be	-	<0.0003	0.1	<0.0003					
others	0.15	<0.05	0.15	<0.05					
Al	balance							3	4.4-5.4
C					≤0.12	≤0.08	0.08		
P					≤0.045	≤0.03			
S					≤0.045	≤0.03			
$R_{p0.2}$/MPa	145	110	125	40	170	170	440	170	125
R_m/MPa	300	240	235	120	<440	<400	530	240	230
A_5/%	22	17	23	8	28	33	30	17	10

covers from 12 mm to 15 mm. The contact point of the welding wire at the lower sheet for all the material combinations is about 1.5 mm away from the fillet weld root.

For all the welding experiments optimised parameters were used to get good wetting at the weld flank. For AW5083-O and AW6181-T4 the welding parameters refer to Kerschbaumer[13]. The fillet welds of deep-drawing steels were welded utilising the optimised parameter sets of the company ACC Austria for the 30 mm/s weld speed. For the Al und Mg experiments the welding speed of 15 mm/s was selected. The forehand angle α varied between 0° (AW5083-O, AZ31) and 5° (AW6181-T4, DD11 and DD13). The shielding gases of 50 : 50 Ar and He and Corgon 18 (which is 18 : 82 CO_2 and Ar) were used for Al, Mg and steel welding. The energy input varied between 0.9 kJ/cm (AZ31) and 3.4 kJ/cm (DD13). Aluminium and DD11 were welded with a similar energy input. All the welding parameters are listed in **Table 2**.

2.2.2 Tensile and corrosion tests

From the welded overlap joints the 50 mm × 180 mm samples for corrosion and shear tests as well as metallographic investigations were prepared and the 50 mm × 100 mm ones were prepared from the base materials, **Figure 2**. The shear strength of the joints was tested according to EN ISO 9018:2006[14] utilizing a Zwick RMC100 tensile-testing machine. The free clamping length was adjusted to 120 mm. The strain rate (traverse speed) was 2 mm/min at room temperature. For comparability, the measured fracture forces were converted to the tensile strength (50 mm sample width, 3 mm or 2.5 mm sheet thickness). The arithmetic mean and the standard deviation have been calculated for each sample.

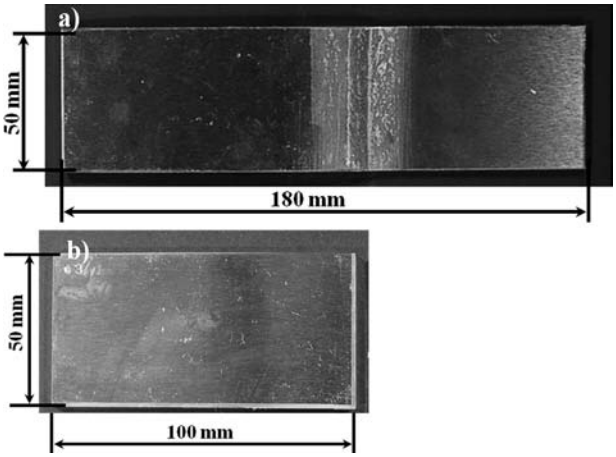

Figure 2: Corrosion samples; a) welding joint for tensile-shear test and metallography; b) base material
Slika 2: Vzorci za korozijo; a) varjeni spoj za natezni strižni preizkus in metalografijo; b) osnovni material

The corrosion resistance of the welded joints and base materials was investigated using the neutral salt spray test (NSS) according to EN ISO 9227:2006[15] as well as the fruit acid spray test (FS) according to DIN 8985.[16] Corrosion testing was performed using a Köhler corrosion chamber HKT500. The samples were taken out after (2, 6, 24, 48, 96, 168, 240 and 480) h, documented macroscopically with a digital reflex camera Nikon D50 and the mass gain was determined with a scale of the company Denver Instrument MXX-612 with an accuracy of 0.01 g, according to DIN 50905-1.[17] Due to a limited number of the samples the determination of the mass loss after removing the corrosion product was not carried out. After 240 h and 480 h metallographic investigations with LOM (Zeiss Z1m) and REM (Zeiss 1415VP) and the tensile-shear tests were performed to detect the impact of corrosion on the weld strength.

Table 2: Welding parameters for the selected material combinations/TPS 4000/CMT
Tabela 2: Parametri varjenja za izbrane kombinacije materialov /TPS 4000/CMT

Base material	AW5083-O	AW6181-T4	DD11	DD13	AZ31
Filler metal	AlMg5	AlSi5	EMK6	EMK6	AM50
Current type	Pulse	Pulse	Pulse	Standard	CMT+P
Sheet thickness (mm)	3	2.5	3	3	3
Shielding gas/quantity (L/min)	50 : 50 Ar:He 17	50 : 50 Ar:He 17	Corgon 18 18	Corgon 18 18	50 : 50 Ar:He 17
rapdefaultWire feed drive (m/min)	7.1	5.8	7.5	11.5	11
Voltage *U*/V	19	24.6	23.3	29.4	12.3
Current *I*/A	123	113	244	344	113
Welding speed *v*/(mm/s)	15	15	30	30	15
Energy input *E*/(kJ/cm)	1.55	1.85	1.90	3.37	0.93
Comments	α = 0° β = 50°	LBK -2 α = 5° forehand β = 50°	α = 5° forehand β = 50°	α = 5° forehand β = 50°	LBK-1 α = 0° β = 50°

3 RESULTS

3.1 Theoretical background

3.1.1 Deep-drawing steel

In saline solutions or brines, uniform- or shallow-pitting corrosion occurs, and occasionally there is also pitting corrosion, if chloride is deposited locally.[18–20] In the seawater with a salt concentration of about 29.2 g/l shallow pitting or pitting corrosion appears on deep-drawing steel. In the hydrochloric acid the corrosion rate increases linearly with the temperature and acid concentration.[18,20] In organic acids iron is corrosion resistant as long as the access to oxygen is prohibited. Generally, the uniform corrosion attack increases with an increase in the organic-acid concentration.[18,20]

3.1.2 Aluminium

In the atmosphere the less noble aluminium (with an electrochemical potential of –1.66 V) forms an Al_2O_3 dense oxide layer. This oxide layer causes a chemical resistance in the pH range of 4.5 to 8.8. For lower and higher pH values, i.e., for acidic or alkaline attacks the passive layer is dissolved and a uniform corrosion takes place. In chloride media aluminium shows pitting, intergranular corrosion and stress-corrosion cracking. In drinking water aluminium and Al_2O_3 are resistant unless the Al_2O_3 layer is mechanically damaged, e.g., due to grinding.[18,19,21–25] In milk aluminium forms an oxide layer with a good resistance. It is attacked by salt, hydrofluoric acid and alkali.[18]

Aballe has found in his work that precipitates [Al(Mn, Fe, Cr) and Al(Si, Mg)] cause the pitting in AW5083-O. The precipitates Al(Mn, Fe, Cr) are more noble than the base material matrix and the corrosion takes place in the Al matrix.[26,27]

An intergranular corrosion attack is formed along the Mg_2Si precipitates at the grain boundaries in AW61814-T4. The following precipitates stimulate an intergranular corrosion attack: $CuAl_2$ in 2xxx[28], Mg_2Al_3 in 5xxx[25], $MgZn_2$ in 7xxx[25] and Mg_2Si[29] or $CuAl_2$[28] in 6xxx. There are two types of intergranular corrosion, dependent on the nobility of the grain boundaries. The less noble Al_8Mg_5 precipitates in the 5xxx alloys[30,31] and the $MgZn_2$ precipitates in the 7xxx alloys are dissolved anodically. With the more noble grain-boundary precipitates like Mg_2Si or $CuAl_2$, the surrounding matrix material is dissolved.[18,19,22,24,32–35]

3.1.3 Magnesium

In the chloride-containing atmospheres and in salt solutions magnesium is not resident, as the protective oxide layer MgO is dissolved. In natural brines magnesium-salt crystals are formed that dissolve easily in water. Therefore, no further protective oxide layer is formed because in an aqueous chloride solution the passive layer is dissolved and no other corrosion protection is in place. In neutral media like humid air, MgO is transformed into a protective $Mg(OH)_2$ layer[2]. Manganese and zinc have a positive effect on the corrosion resistance of magnesium, where the Zn content must be below 3 %. When alloying aluminium and magnesium, the corrosion resistance in salt water increases[18,20,21,30,33,36–38].

3.2 Corrosion behaviour in the salt spray and fruit acid tests

Macroscopically a distinct difference in corrosion behaviour between the welded and base-material sheets is visible if the NSS and FS tests are compared. The steel sheets show a relatively thick rust layer after a 480 h NSS test, whereas after a FS test only a slight rust layer can be seen. It is noticeable that during the FS test rust layers are formed only on the welded steel joints, not on their base sheets. In the case of magnesium pitting can be seen macroscopically after the NSS and FS tests. In the case of aluminium both AW5083-O and AW6181-T4 show formations of white corrosion products (aluminum hydroxide) during the NSS and FS tests and they are more distinctive for the latter (**Figures 3a** and **b**).

3.2.1 Salt spray test (NSS) – metallographic investigations

3.2.1.1 Base materials

After 480 h, on the AW5083-O surface, a few small pitting sites could be detected with a stereo microscope (**Figure 4a**), while AW6181-T4 showed no pitting. Both alloys were covered with white corrosion products that were more pronounced on AW6181-T4, **Figure 4b**. The steel and magnesium sheets showed strong corrosion

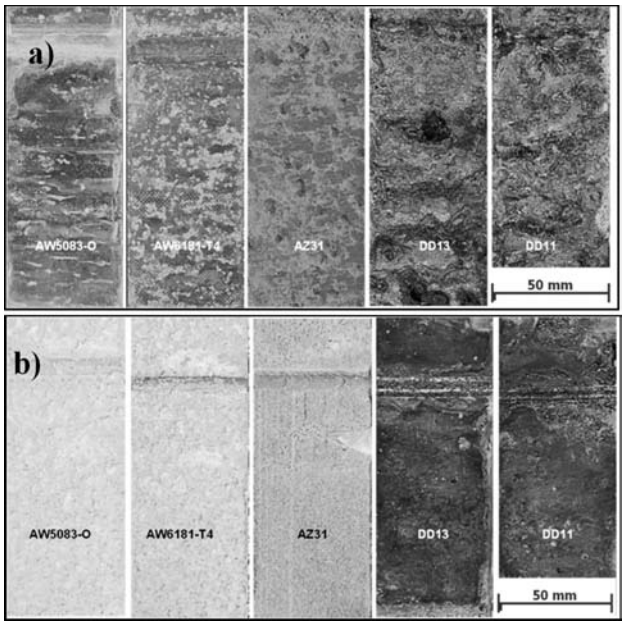

Figure 3: Corrosion samples after 480 h: NSS test (left), FS test (right)

Slika 3: Vzorci s korozijo po 480 h: NSS-preizkus (levo), FS-preizkus (desno)

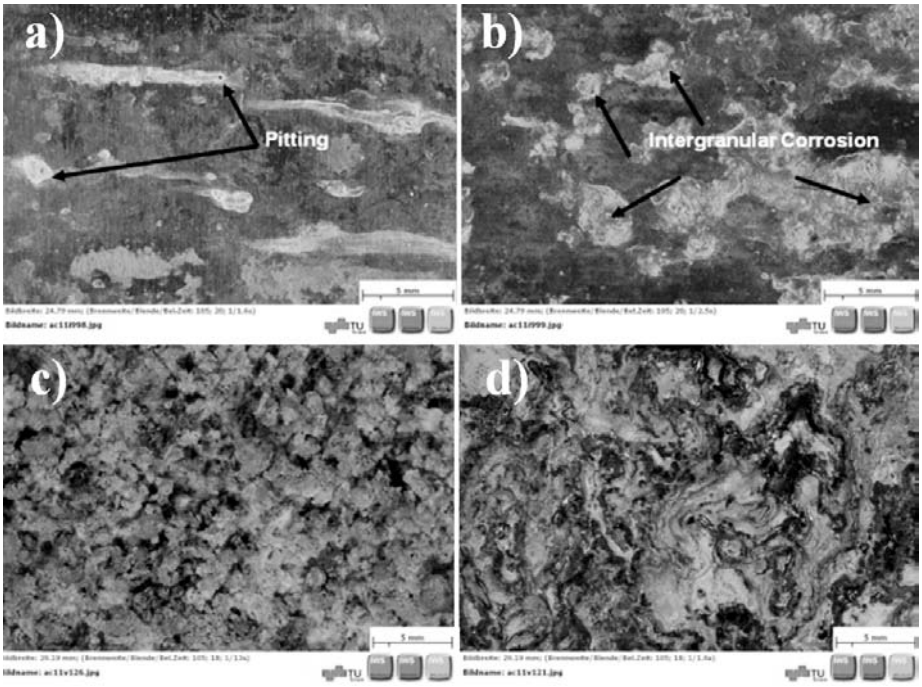

Figure 4: Corrosion after the NSS test/surfaces shown with a stereo microscope: a) AW5083-O, 480 h, b) AW6181-T4, 480 h; c) AZ31, 240 h; d) DD11, 240 h

Slika 4: Korozija po NSS-preizkusu; površine, prikazane s stereomikroskopom: a) AW5083-O, 480 h, b) AW6181-T4, 480 h; c) AZ31, 240 h; d) DD11, 240 h

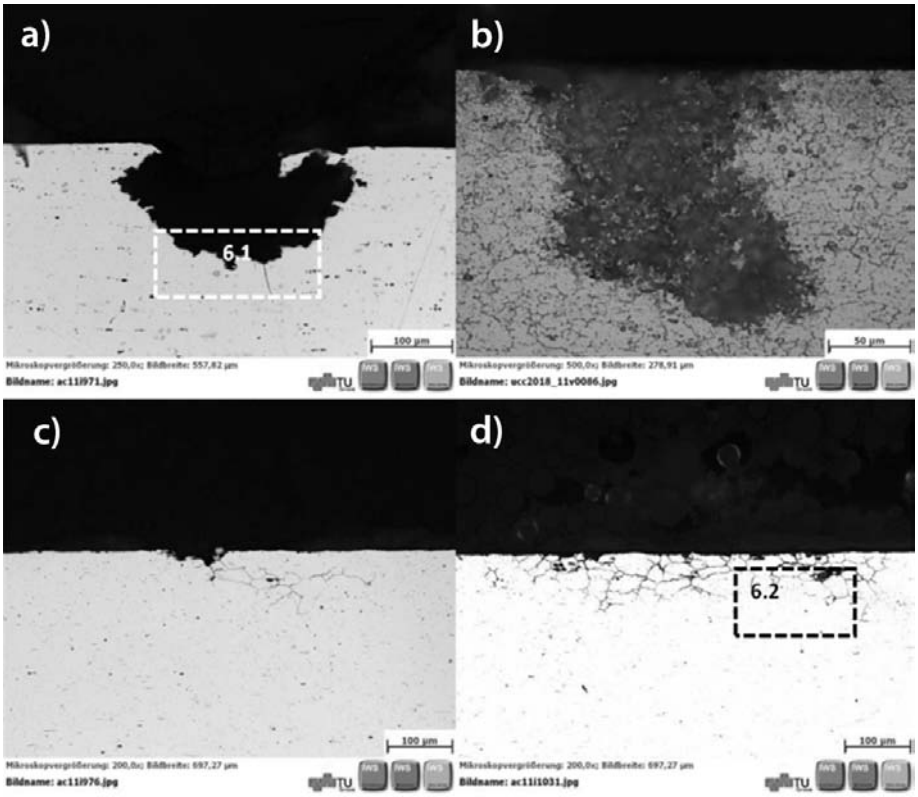

Figure 5: Corrosion after the NSS test/cross-section details in LOM: a) AW5083-O, 240 h; b) AW5083-O, 480 h; c) AW6181-T4, 240 h; d) AW6181-T4, 480 h

Slika 5: Korozija po NSS-preizkusu; detajli prereza, svetlobna mikroskopija (LOM): a) AW5083-O, 240 h; b) AW5083-O, 480 h; c)AW6181-T4, 240 h; d) Aw6181-T4 po 480 h

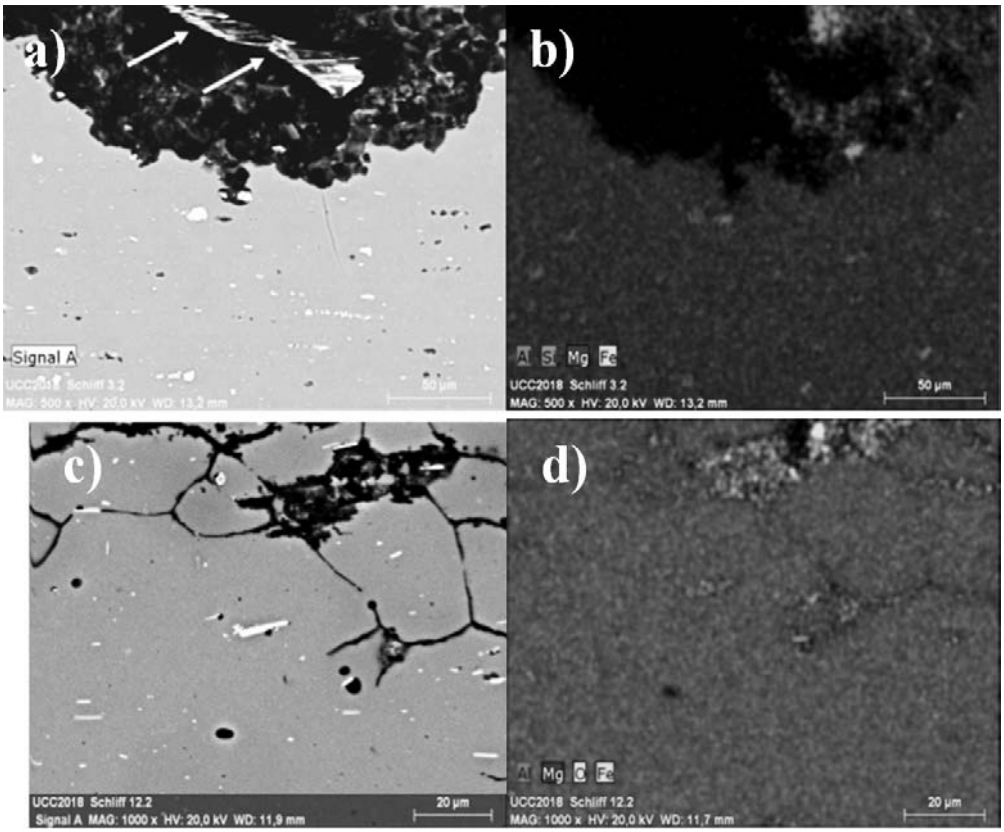

Figure 6: SEM and EDX of **Figure 5:** a) and b) AW5083-O, detail 6.1; c) and d) AW6181-T4, detail 6.2
Slika 6: SEM- in EDX-posnetka področij na **sliki 5**: a) in b) AW5083-O, detajl 6.1; c) in d) AW6181-T4, detajl 6.2

already after 240 h. On the AZ31 sheet, a porous white corrosion product was formed, **Figure 4c**. The steels show abundant red rust, whereat the first signs of corrosion occurred already after a few hours, **Figure 4d**.

The cross sections confirm the pitting corrosion for the AW5083-O alloy observed after 168 h with the stereo microscope. Significant pits were found after 240 h. **Figure 5a** shows a pit depth of about 0.16 mm observed with a light optical microscope (LOM). Primary precipitates and impurities containing Fe, Si and Mg were detected at the bottom of the pit with an energy-dispersive X-ray analysis (EDX) using a scanning electron microscope (SEM), **Figures 6a** and **b**. These precipitates behave electrochemically nobler and get exposed to the corrosion. The pitting progress into the depth from 240 h to 480 h is marginal (**Figure 5b**). The AW6181-T4 alloy shows intergranular corrosion (IG) starting in the small pitting areas and reaching a depth of about 0.1 mm (**Figures 5c** and **d**). The corrosion progress from 240 h to 480 h shows no further increase in the depth but spreading. The first superficial corrosion attack was visible already after 2 h. On closer examination, primary

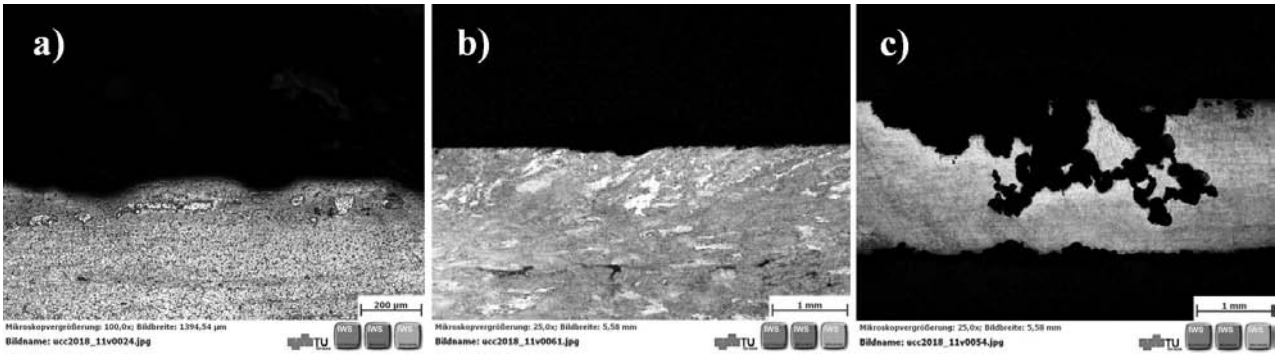

Figure 7: Corrosion after 480-h NSS/base-material cross sections in LOM: a) DD11 – uniform corrosion and shallow pitting; b) AZ31 grinded sample – uniform corrosion; c) AZ31 non-grinded sample – severe corrosion attack
Slika 7: Korozija po 480 h NSS; prerez osnovnega materiala, svetlobna mikroskopija (LOM): a) DD11 – enakomerna korozija in plitve jamice; b) AZ31 brušeno – enakomerna korozija; c) AZ31 nebrušeno – resen pojav korozije

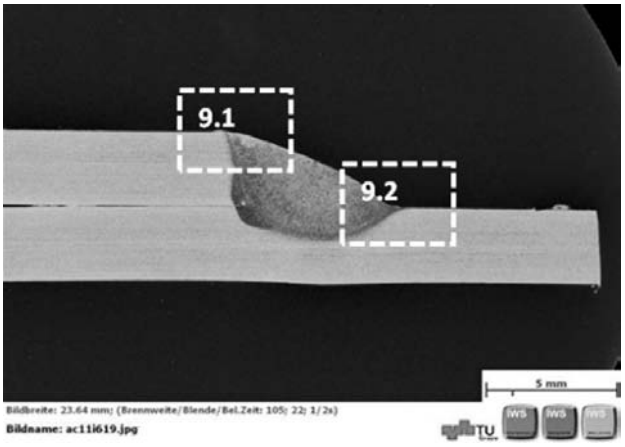

Figure 8: AW5083-O welded joint/fillet-weld cross section in LOM prior to the NSS test; hydrofluoric acid/alcoholic etchant
Slika 8: AW5083-O varjeni spoj; prerez zvara, svetlobna mikroskopija LOM pred NSS-preizkusom; kislina HF in alkoholno jedkalo

precipitates could be detected. In the SEM investigations no secondary phases (T4 aged) could be found, **Figures 6c** and **d**.

The cross section of the DD11 steel shows uniform corrosion and shallow pitting. It can be expected that DD13 has a similar corrosion behaviour, **Figure 7a**.

The magnesium alloy AZ31 exhibits a strong dependence on the initial surface roughness. Generally, the grinded samples have uniform corrosion and shallow pits, which are then fortified in depth. But the non-grinded AZ31 samples show a very strong local-corrosion attack combined with uniform corrosion. After 480 h almost the entire 3-mm sheet was dissolved, i.e., corroded as seen in **Figures 7b** and **c**. This significant difference can be attributed to the effect that a corrosive medium adheres less on the surfaces with low roughness.

3.2.1.2 Welded joints

In general, no effect of the used welding parameters on the corrosion behaviour was detected, compare[13]. The corrosion attack after 480 h was analyzed in the cross sections of the fillet welds, **Figure 8**.

Pitting corrosion occurred at the heat affected zone (HAZ) of alloy AW5083-O and in the AlMg5 weld metal. At the weld edges and the fusion line, local corrosion was detected, too. Furthermore, the surface pores in the AlMg5 weld metal were found to be the starting points for pitting and crevice corrosion as seen on **Figure 9**, compare.[13]

Sanchez-Amaya[39] also found this corrosion behaviour with the corrosion tests involving a mixture of NaCl and H_2O_2. In the investigations of Mutombo in 2011[40], AW5083-O was MIG-welded with both filler metals, AlMg5 and AlSi5, to a Y-joint and tested in 3 % NaCl. He traced the corrosion start back to the existing surface pores. The tough AlMg5 weld and HAZ showed pitting.

The AW6181-T4 welded joints showed no corrosion at the fusion line or on the AlSi5 weld metal.

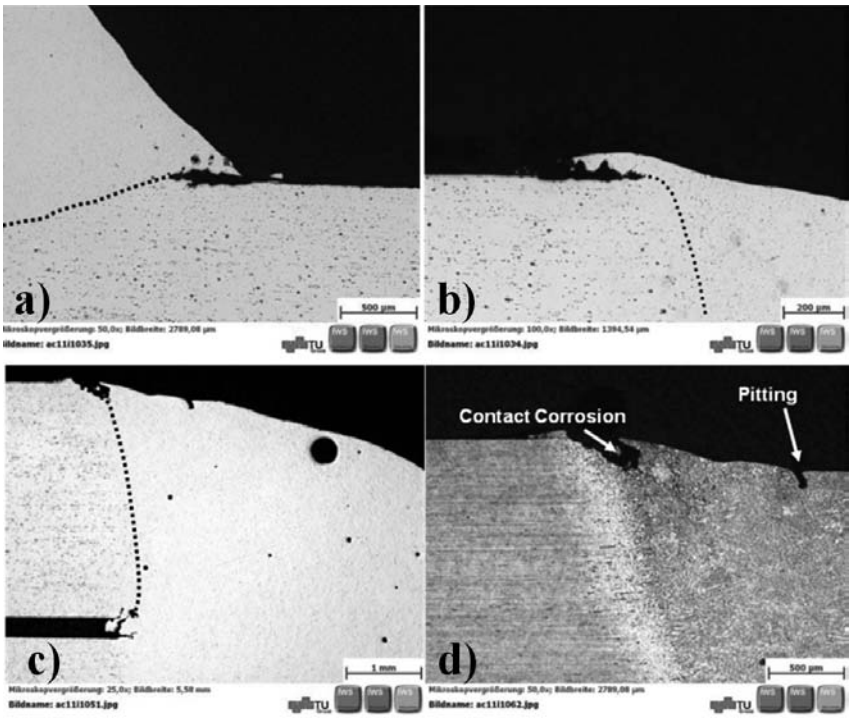

Figure 9: Welded AW5083-O joint cross sections in LOM/corrosion after the 480 h NSS test/local corrosion at the fusion line and weld-metal surface pores: a)–d) details 9.1 and 9.2 from **Figure 8**
Slika 9: Svetlobna mikroskopija (LOM) prečnega prereza zvara AW5083-O; korozija po 480 h NSS-preizkusa; lokalna korozija na liniji taljenja in pore na površini materiala zvara: a)–d) detajli 9.1 in 9.2 s **slike 8**

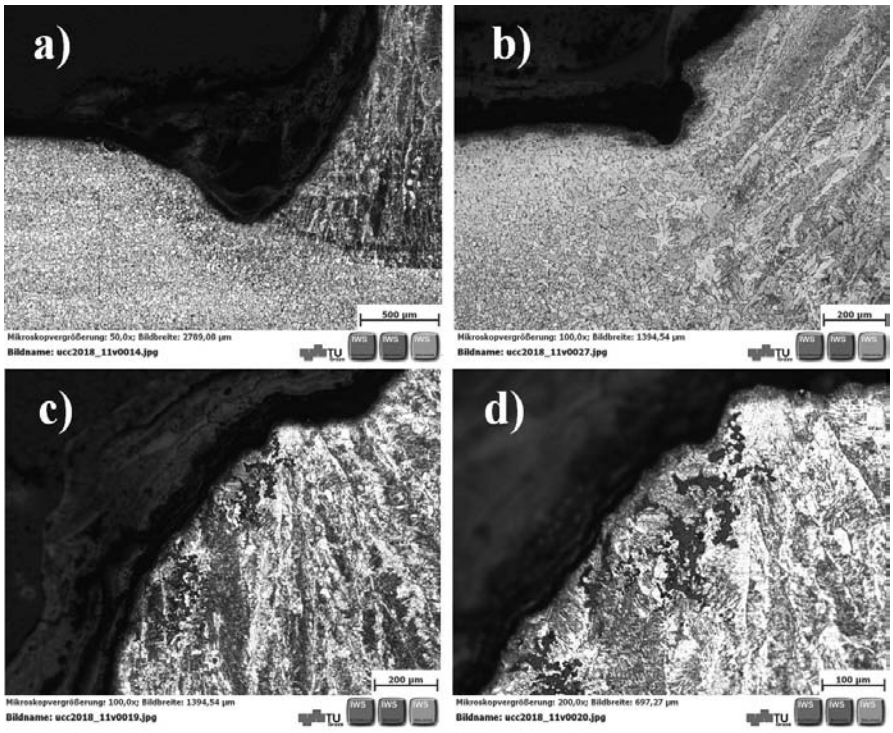

Figure 10: Welded steel-joint details – cross sections in LOM/corrosion after the 480 h NSS test/local corrosion at the fusion line: a) DD11; b) DD13; c and d) G3Si1 weld metal

Slika 10: Detajli zvarjenega spoja jekla – prečni prerez s svetlobno mikroskopijo (LOM); korozija po 480 h NSS-preizkusa; lokalna korozija na liniji taljenja: A) DD11; b) DD13; c) in d) G3Si zvarjena kovina

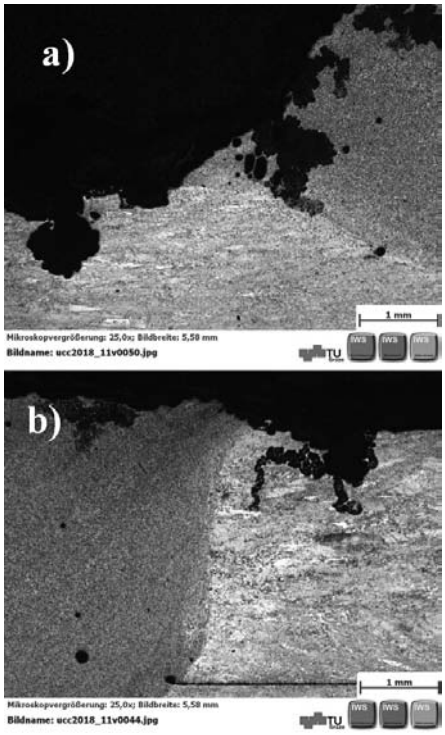

Figure 11: Welded AZ31 joint, grinded – cross sections in LOM/corrosion after the 480 h NSS test: a) lower weld edge; b) upper weld edge – strong corrosion of the AM50 weld metals and the base metal

Slika 11: Zvarjen AZ31 spoj, brušeno – prečni prerez, svetlobna mikroskopija LOM; korozija po 480 h NSS-preizkusa: a) spodnji rob zvara, b) zgornji rob zvara – močna korozija AM50 zvarjene kovine in osnovnega materiala

The welded steel joints showed an intense corrosion attack along the fusion line and selective corrosion of the G3Si1weld metal, **Figures 10a** to **d**.

The AZ31 welded joints were manufactured only from the grinded magnesium alloy and were NSS tested. **Figures 11a** and **b** shows strong and partially localized corrosion on the AM50 weld metal as well as on the base material. Obviously, the bottoms of the formed cavities (large pits) act as starters for more pitting corrosion progressing into the depth.

3.2.2 Fruit acid test (FS) – metallographic investigations

3.2.2.1 Base materials

For AW5083-O, pitting corrosion of about 0.1 mm in depth occurred after the 240 h FS test. Continuing the corrosion test to 480 h, the pits did not progress in depth but grew wider, to about 0.6 mm, **Figures 12a** and **b**. This was caused by an electrolytic dissolution of metal in an acidic medium, compare.[10] In contrast, AW6181-T4 shows intergranular corrosion after 240 h (0.15 mm deep), just slightly progressing in depth (0.18 mm) during the 480 h FS test. However, the IG corrosion spread by about 2–3 mm in width after 480 h, **Figures 12c** and **d**.

The DD11-steel base material exhibits pitting corrosion after the 240 h and 480 h FS tests. In the etched cross section, partial IG corrosion could be found, too, **Figures 13a** to **c**. The results of the corrosion

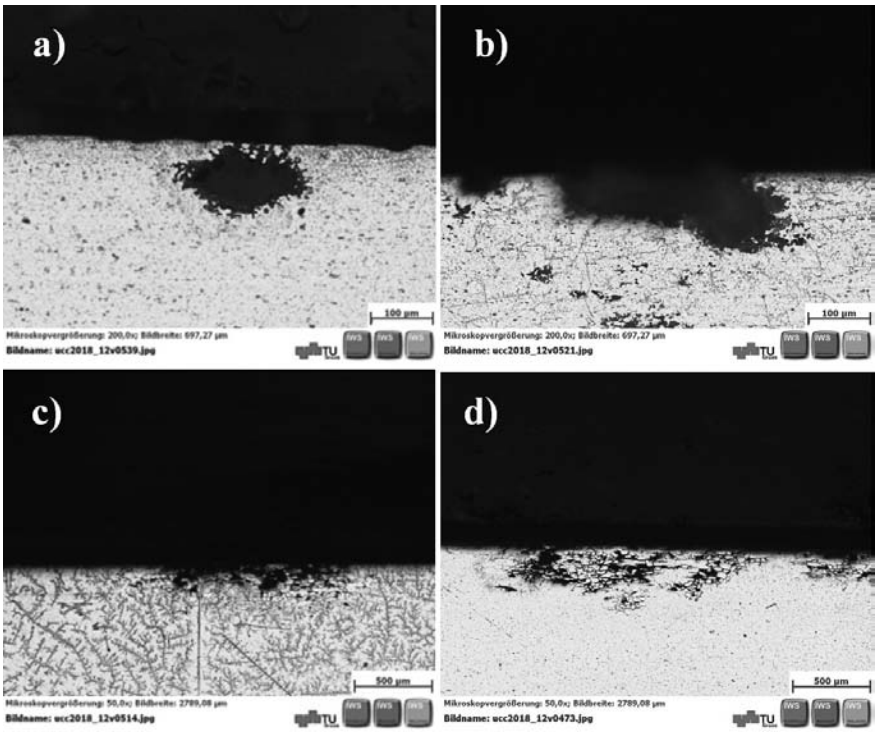

Figure 12: Corrosion after the FS test/cross-section details in LOM: a) AW5083-O, 240 h; b) AW5083-O, 480 h; c) AW6181-T4, 240 h; d) AW6181-T4, 480 h

Slika 12: Korozija po FS-preizkusu; detajli prečnega prereza s svetlobno mikroskopijo (LOM): a) AW5083-O, 240 h; b) AW5083-O, 480 h; c) AW6181-T4, 240 h; d) AW6181-T4, 480 h

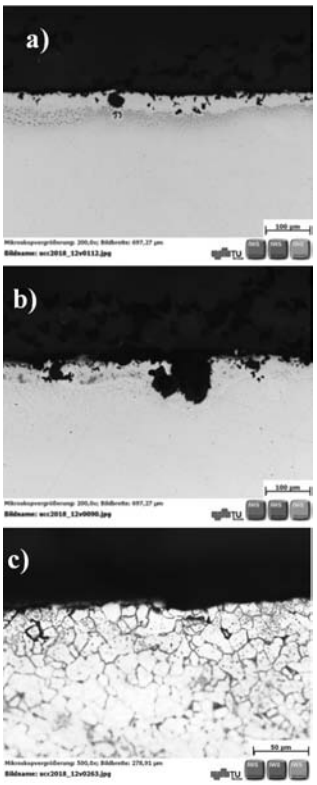

Figure 13: Corrosion of DD11 steel after the FS test/cross-section details in LOM: a) 240 h; b) 480 h; c) 480 h, etched with Nital

Slika 13: Korozija DD11 jekla po FS-preizkusu; detajli prečnega prereza, svetlobna mikroskopija (LOM): a) 240 h; b) 480 h; c) 480 h, jedkano z nitalom

behaviour of the DD13-steel base material are quite similar to the DD11 results.

The grinded AZ31 magnesium base material shows shallow pitting after the 240 h FS. Contrary to the NSS, during the 480 h test the corrosion progresses strongly, whereat localized corrosion and pitting arise, especially at the backside of the sample, **Figures 14a** and **b**.

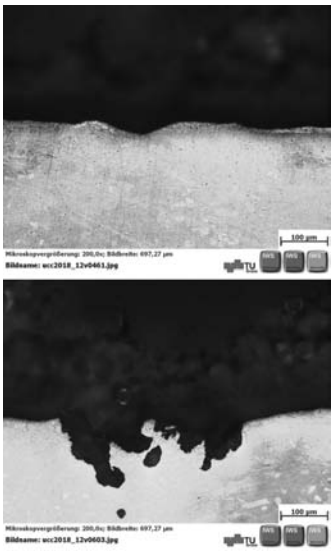

Figure 14: Corrosion of AZ31 after the FS test/cross-section details in LOM: a) 240 h; b) 480 h

Slika 14: Korozija AZ31 po FS-preizkusu; detajli prečnega prereza, svetlobna mikroskopija (LOM): a) 240 h; b) 480 h

3.2.2.2 Welded joints

After the 240 h FS test, alloy AW5083-O exhibits pitting corrosion at the fusion line and on the base material. After 480 h distinct pitting is found in the AlMg5 weld metal, too. At the weld edges a strong localized corrosion attack is found along the marked fusion line, whereat the corrosion depth remained to be about 0.8 mm between 240 h and 480 h, **Figures 15a** to **c**.

The welding joint AW6181-T4 does not lead to the corrosion of the weld edges or the AlSi5 weld metal. Here the IG corrosion is found on the base material as shown in **Figures 12c** and **d**.

After the 240 h FS test, the welded DD11-steel joint shows local corrosion at the weld edges. The shallow-pitting corrosion in the G3Si1 weld metal can be seen after 480 h, **Figures 16a** and **b**. These results are similar to the ones for the NSS test, **Figure 10a**.

In the AM50 weld metal of the AZ31 magnesium joint, a notable amount of pores appeared. They had no significant influence on the corrosion behaviour during the FS test. **Figures 17a** and **b** shows shallow pitting corrosion as well as crevice corrosion at the cold weld edge after 240 h. These results are less critical than those related to the strong localized corrosion in the NSS test.

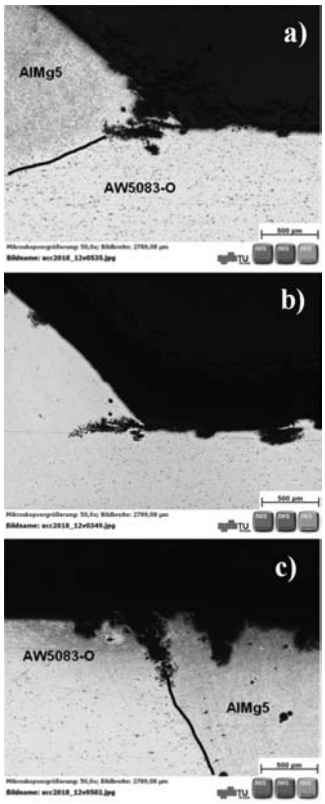

Figure 15: Welded AW5083-O joint cross sections in LOM/corrosion after the FS test: a) 240 h; b) 480 h, lower weld edge; c) 480 h, upper weld edge (see **Figure 8**)

Slika 15: Prečni prerez zvarjenega spoja AW5083-O, svetlobna mikroskopija (LOM); korozija po FS-preizkusu: a) 240 h; b) 480 h, spodnji rob zvara; c) 480 h, zgornji rob zvara (glej **sliko 8**)

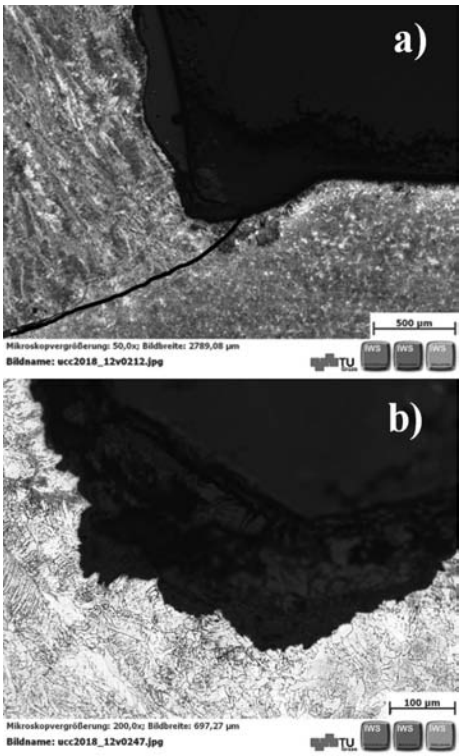

Figure 16: Welded DD11-steel joint details – corrosion after the FS test: a) 240 h; b) 480 h, G3Si1 weld metal

Slika 16: Detajli zvarjenega spoja DD11-jekla; korozija po FS-preizkusu; a) 240 h; b) 480 h G3Si1 zvar

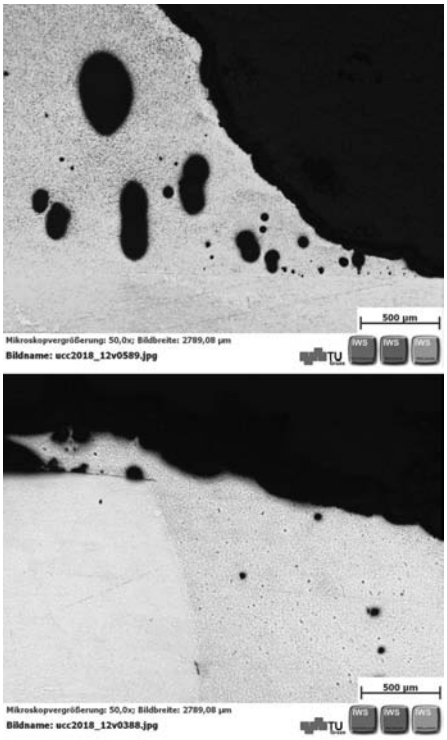

Figure 17: Welded AZ31 joint, grinded – AM50 weld metal details/ corrosion after the 240 h NSS test: a) lower weld seam; b) upper weld seam

Slika 17: Spoj zvarjenega AZ31, brušeno – detajl AM50 zvara; korozija po 240 h NSS-preizkusa: a) spodnji šiv zvara; b) zgornji šiv zvara

3.3 Corrosion influence on the welded-joint strength

The tensile-shear test results before and after the corrosion testing are shown in **Figures 18a** and **b**. The fracture forces were recorded and standardized with the initial cross-sectional area (50 mm × 3 mm and 50 mm × 2.5 mm for AW6181-T4). The fracture location for all the welded shear- test samples runs along the fusion line. In the as-welded condition, the DD11 and DD13 steels had the highest weld strength (352 MPa and 298 MPa). The difference is due to the lower carbon content of DD13. AW5083-O samples show a weld strength of 274 MPa and AW6181-T4 a strength of 113 MPa. Magnesium AZ31 has the lowest weld strength that is 104 MPa. Considering the influence of the corrosion time and corrosive medium, the following can be observed:

NSS test

The DD13-steel weld showed a 12 % drop in the strength, to 309 MPa, and the DD11 weld strength depletes even by 26 %, to 222 MPa, after the 480 h NSS test. In contrast, no loss in the strength was found for both aluminium alloys. Due to the severe corrosion attack, the strength of the magnesium AZ31/AM50 weld joint decreased significantly, by 78 %, down to 23 MPa, **Figure 18a**.

FS test

The DD11-steel weld strength decreased to a value of 331 MPa (–6 %). However, for DD13 no loss of strength was detected. Also, for the AW5083-O/AlMg5 and AW6181-T4/AlSi5 weld joints no effect of corrosion occurred after 480 h. The weld strength of AZ31 decreased sharply to 62 MPa (–40 %), **Figure 18b**.

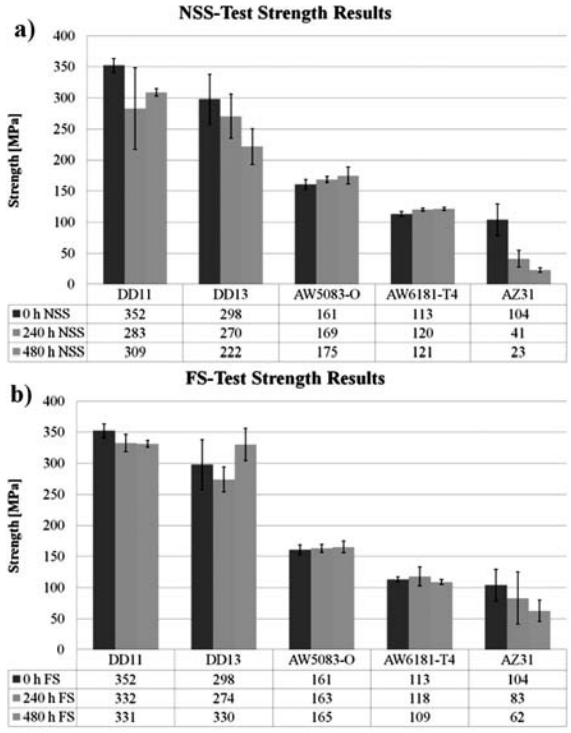

Figure 18: Welded-joint strength over the corrosion testing time; a) NSS; b) FS test

Slika 18: Trdnost zvarjenega spoja v odvisnosti od časa korozijskega preizkušanja; a) NSS-; b) FS-preizkus

3.4 Approximation of the base-material-corrosion mass losses and rates

Weight measurements were performed on the 50 mm × 100 mm base-material samples, see results in **Figure 19**. To calculate the mass loss per unit area (g/m^2) Formula 1 was used. Therefore, the chemical composition of the resulting corrosion products (Me_nX_m) on the sample surfaces must be known. Their respective compositions from the literature are Fe_2O_3 for iron[41], Al_2O_3 for aluminum[10,42] and $Mg(OH)_2$ for magnesium[8]. According to DIN 50905, part 2[43], the mass loss per unit area and the corrosion rate can be calculated for the supposed uniform surface corrosion. It must be noted that the aluminum samples showed irregular or localized corrosion. For pitting corrosion, selective corrosion and intergranular corrosion, DIN 50905, Part 3[44] describes the evaluation of the corrosion samples by determining the thinning. But in order to obtain comparability for all the tested materials, a simplified uniform surface corrosion was presumed. Applying Formula 2 and Formula 3, the material-loss rates can be calculated[43]. The mass-loss rate per unit area was calculated with difference m_a from mass loss m_a at time t_n reduced by the mass loss of the previous evaluation time $t_{(n-1)}$.

$$m_a = \frac{-\Delta m}{A} = \frac{+\Delta m}{A} \cdot \frac{n \cdot A_{r,Me}}{m \cdot A_{r,X}}$$

Formula 1: Mass loss per unit area [17]

$$v_{diff} = \frac{dm_a}{dt}$$

Formula 2: Mass-loss rate per unit area (g/m^{2}h) [43]

$$w_{diff} = 8.76 \cdot \frac{v_{diff}}{\rho}$$

Formula 3: Corrosion rate (mm/a) [43]

Legend:

m_a… Mass loss per unit area (g/m^2)
$-\Delta m$… Mass loss (g)
$+\Delta m$… Mass increase (g)
A… Surface (m^2)
$n*A_{r,Me}$… n · relative atomic mass of corrosion product Me_nX_m
$m \cdot A_{r,X}$… m · relative atomic mass of non-metal X (oxygen) in composition Me_nX_m
v_{diff}… Mass loss rate per unit area (g/m^{2}h)
dm_a… Differential mass loss per unit area (g/m^2)
dt… Differential time between single tests (h)
ρ… Base material density (g/cm^3)

The calculation results are the following:

3.4.1 NSS test

In **Figure 19a** the mass gains of all the examined materials during the period of 480 h are shown. Four samples were evaluated for each base material. Non-grinded magnesium AZ31 (line 6) initially shows the highest mass increase. After 240 h the mass decreases due to the loss in the corrosion product. The mass increase in the grinded AZ31 samples (line 5) is much lower and even below the steel mass increase. The DD11 (line 3) and DD13 (line 4) steels show the same mass gain up to 96 h. Thereafter, DD13 corrodes more significantly. Aluminium AW5083-O (line 1) and AW6181-T4 (line 2) tend towards pitting and intergranular corrosion, causing very low mass gains.

3.4.2 FS test

In **Figure 19b** the mass loss over the testing time for all the tested materials is exhibited. It can be seen that AZ31 (line 5) and DD13 (line 4) are forming adherent corrosion layers up to 2 h. All the other materials (AW6181-T4, AW5083-O and DD11) show neither an increase nor a decrease. Up to 24 h all the samples gain weight due to the formation of corrosion products. Afterwards, until the test end, a steady weight loss for all the samples is observed (except for the AW5083-O increase up to 48 h). After 48 h steels DD11 (line 3) and DD13 (line 4) sustain a strong weight loss, i.e., approximately 1.25 g. By comparison, the 0.3 g weight losses in the aluminium alloys are quite low. The weight loss in AZ31 after 480 h amounts to 0.45 g. While drying the AZ31 samples, flaky corrosion products fall off the samples that cannot be included in the mass loss.

3.4.3 Mass loss per unit area – the NSS test

The standardized mass losses after 240 h for steels DD13 (1250 g/m^2 – line 4), DD11 (1000 g/m^2 – line 3) and non-grinded magnesium AZ31 (800 g/m^2 – line 6) progress relatively linear, **Figure 20a**. At 480 h the corrosion for DD11 decreases stronger than for DD13. Non-grinded AZ31 shows a negative mass loss after 480 h due to the corrosion product falling off. The grinded AZ31 (line 5) shows a constant and much lower mass loss of just corrosion until the test end, whereat the corrosion product adheres on the sample due to the low surface roughness. AW5083-O (line 1) and AW6181-T4 (line 2) show a very low mass loss as expected.

3.4.4 Mass loss per unit area – the FS test

Figure 20b shows that steels DD11 (line 3) and DD13 (line 4) have the highest mass loss. From 96 h onwards the loss increases quite linearly up to approximately 240 g/m^2 after 480 h. For the materials AW6181-T4 (25 g/m^2), AW5083-O (50 g/m^2) and AZ31 (87 g/m^2) the mass loss is considerably lower.

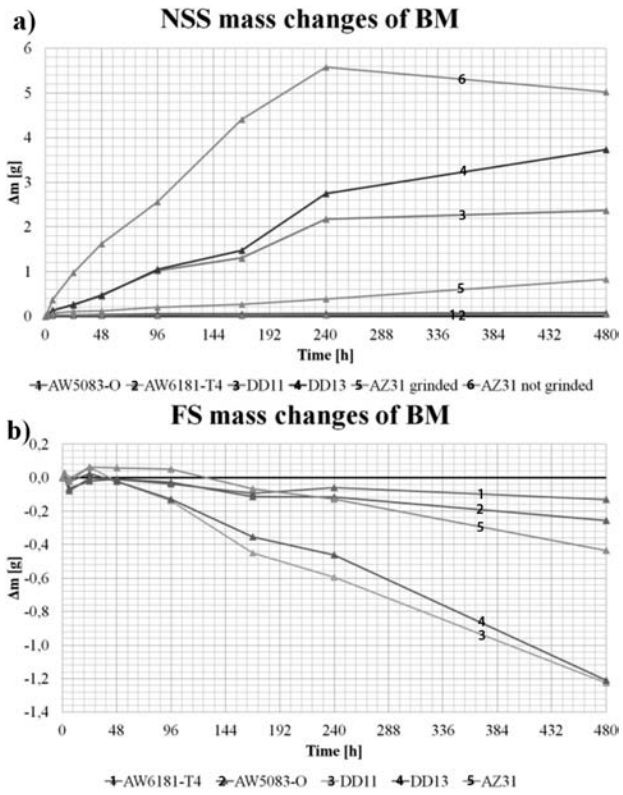

Figure 19: Base-material mass changes over the 480 h test period, a) NSS test b) FS test

Slika 19: Spreminjanje mase osnovnega materiala med preizkusom 480 h, a) NSS-preizkus b) FS-preizkus

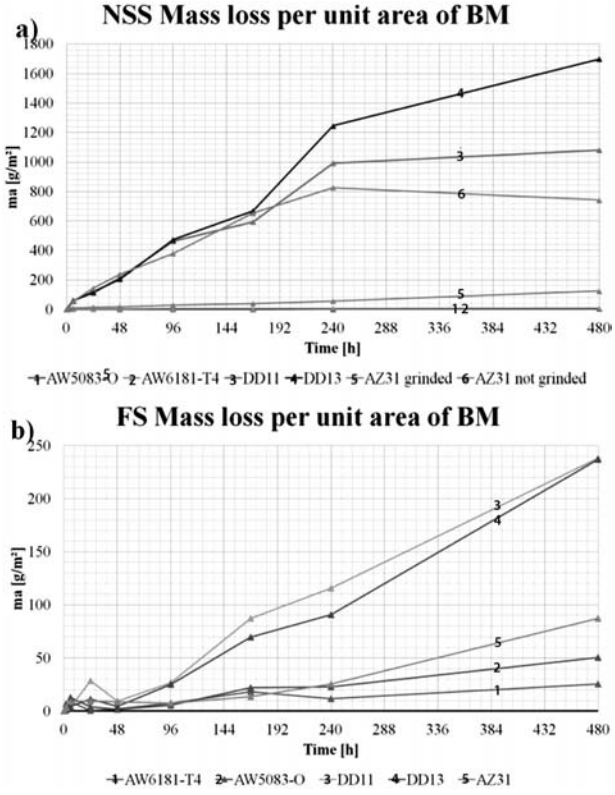

Figure 20: Mass loss per unit area over the 480 h test period: a) NSS test, b) FS test

Slika 20: Zmanjšanje mase na enoto površine med preizkusom 480 h; a) NSS-preizkus, b) FS-preizkus

3.4.5 Corrosion rate – the NSS test

For the steels at the beginning of the NSS test, the corrosion rates are quite high, i.e., around 12 mm per year at instant 6 h. The non-grinded magnesium AZ31 exhibits a tremendous corrosion rate of 52 mm per year, but the grinded AZ31 shows just 8.4 mm per year. To the contrary, the aluminium alloys show low or immeasurable corrosion rates (AW6181-T4: 2.2 mm per year; AW5083-O: 0.0 mm per year) at instant 6 h. By continuing the test, the corrosion rates decrease more or less to 240 h and fall down further at instant 480 h for all the materials, **Figure 21a**. The reason for these materials' passivation is probably the adherent corrosion products on the sample surfaces acting as corrosion barriers. At the end of the NSS test, the steels (0.6 and 2 mm per year for DD11 and DD13) have the highest and the aluminium alloys (AW5083-O and AW6181-T4, each having 0.04 mm per year) the lowest corrosion rate, see **Table 3**.

3.4.6 Corrosion rate – the NSS test

The maximum corrosion rates were found at instant 6 h for AW6181-T4 (13 mm per year), AW5083-O (10 mm per year), AZ31 (5.6 mm per year) and DD13 (0.9 mm per year). Steel DD11 (1.5 mm per year) shows its maximum at instant 24 h. Thereafter, the corrosion rates of the Al and Mg alloys fall significantly and only slightly for the steels. At the end of the FS test AW6181-T4 (0.2 mm per year) and AW5083-O (0.3 mm per year) show the lowest corrosion rate. On the other hand, DD11 (0.5 mm per year) and DD13 (0.7 mm per year) have a significantly higher rate and AZ31 (1.4 mm per year) has the highest rate, **Figure 21b** and **Table 3**.

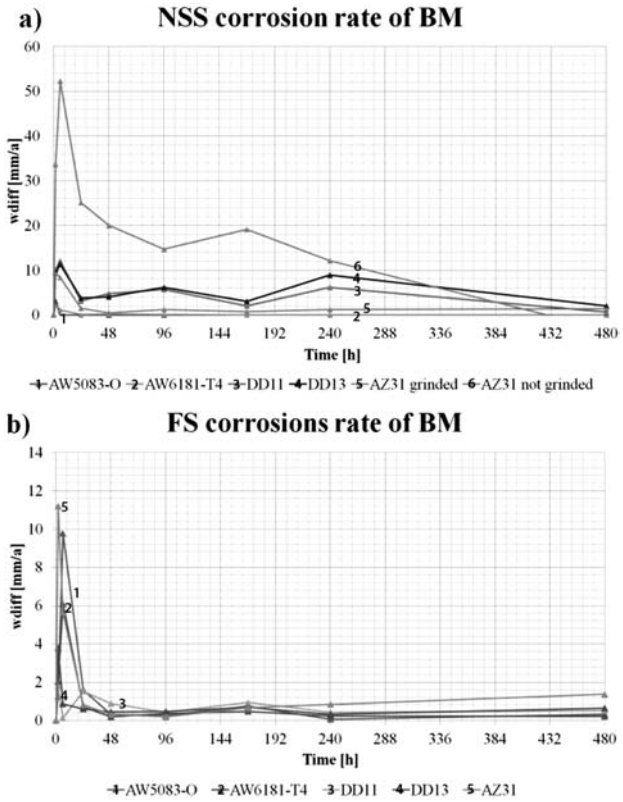

Figure 21: Corrosion-rate behaviour over the 480 h test period: a) NSS test b) FS test

Slika 21: Spreminjanje hitrosti korozije med preizkusom 480 h: a) NSS-preizkus, b) FS-preizkus

4 DISCUSSION

The type of corrosion in the salt spray test (NSS test) and fruit acid test (FS test) is as follows:

Aluminium alloys exhibit localized corrosion. It is notable that the progress in pitting for AW5083-O and intergranular corrosion for AW6181-T4 is reduced during the testing time.

The grinded magnesium alloy AZ31 shows a stronger tendency for localized corrosion in the FS test than in the NSS test. The non-grinded AZ31 is not applicable as a very heavy corrosion attack appears.

The corrosion behaviours of deep-drawing steels DD11 and DD13 are quite similar. In the NSS test mainly uniform corrosion or shallow pitting arises and in the FS test a partial pitting corrosion is observed.

Note that the mass changes due to the corrosion in the NSS test for the steels and magnesium alloy are two to three times higher than in the FS test. Because of the localized-corrosion behaviour of aluminium alloys their mass change is marginal. Similarly, the corrosion rates at certain testing times in the NSS test are multiple compared to the FS test for the steels, **Table 3**.

It is remarkable that in the NSS test adherent corrosion layers are formed on all the materials and the samples gain in weight. In contrast, the corrosion products drain off in the FS test making the samples lose weight.

The corrosion behaviour of the welded joint AW5083-O in the NSS and FS tests is similar. Here the pitting and localized corrosion was found at the fusion line and also at the weld edges on the AlMg5 weld metal. Amazingly, the AW6181-T4 welded joints showed no corrosion at the fusion line or on the AlSi5 weld metal, but just the IG corrosion on the base material.

The corrosion attack on the AZ31 magnesium welded joint was stronger in the NSS test than in the FS. In the former a strong and partially localized corrosion on the AM50 weld metal and on the base material occurred. In the latter only shallow pitting corrosion was found.

The welded steel joints showed an intense corrosion attack at the fusion line in the NSS and FS tests. The corrosion of the G3Si1 weld metal was selective in NSS and took the form of shallow pitting corrosion in the FS test.

The degradation of the tensile-shear strength of the steel welding joints is stronger in the NSS (up to 25 %) than in the FS test. Due to a very high strength loss of the AZ31 magnesium this joint is not applicable. It is a

Table 3: Comparison of the mass-loss rates *v*/(g/(m^2 h)) and corrosion rates *w*/mm per year in the NSS and FS test intervals
Tabela 3: Primerjava hitrosti izgube mase *v*/(*g*/(m^2 h)) in korozijska hitrost *w*/mm na leto pri NSS- in FS-intervalih preizkušanja

Material	Neutral salt spray test (NSS test)						Fruit acid spray test (FS test)					
	96–168		168–240		240–480		96–168		168–240		240–480	
	v g/(m^2 h)	*w* (mm/y)	*v* g/(m^2 h)	*w* (mm/y)	*v* g/(m^2 h)	*w* (mm/y)	*v* g/(m^2 h)	*w* (mm/y)	*v* g/(m^2 h)	*w* (mm/y)	*v* g/(m^2 h)	*w* (mm/y)
DD11	1.80	2.01	5.53	6.16	0.54	0.60	0.84	0.94	0.39	0.44	0.47	0.52
DD13	2.71	3.02	8.01	8.91	1.85	2.06	0.62	0.69	0.29	0.33	0.58	0.65
AW5083-O	0	0	0.02	0.05	0.01	0.04	0.23	0.76	0.02	0.07	0.1	0.33
AW6181-T4	0.01	0.02	0.02	0.07	0.01	0.04	0.15	0.48	0.07	0.24	0.07	0.22
AZ31	0.14	0.73	0.24	1.22	0.27	1.35	0.13	0.66	0.17	0.84	0.27	1.37

benefit of aluminium alloys that they show no influence of corrosion on the welding-joint strength.

5 CONCLUSIONS

Basically, the results of this investigation program allow a technical comparison between the influences of the two relevant corrosion media on the household cooling compressor shells.

The currently used deep-drawing steels cannot be used without an anti-corrosion coating (KTL). Due to a low strength and even a poor corrosion resistance, it is not advisable to use AZ31 as a housing material for household cooling compressors.

The overall result regarding weldability, corrosion resistance and joint strength proves that aluminium alloys can bring improvements to the future compressor shells.

6 REFERENCES

[1] ceced. New EU Energy Labelling and Ecodesign Measures, Brüssel ceced, 2009

[2] Amtsblatt der Europäischen Union, Richtlinie 2010/30/EU des Europäischen Parlaments und des Rates, Brüssel s.n., 2010

[3] Voestalpine, Technische Lieferbedingungen: Weiche, unlegierte Stähle zum Kaltumformen, 2011, www.voestalpine.com/stahl

[4] M. Reuter, Methodik der Werkstoffauswahl- Der systematische Weg zum richtigen Material, Carl Hanser Verlag, München 2007

[5] DVS 0913, DVS Merkblatt 0913, Deutscher Verband der Schweißtechnik, Düsseldorf 1994

[6] J. R. Davis, Aluminum and aluminium alloys, ASM International, vol. 3, Materials Park, Ohio 1994

[7] Böhler welding, Wissenswertes für den Schweißer, Böhler welding, Kapfenberg 09/2010, 2–28

[8] C. Kammer, Magnesium Taschenbuch; 1. Auflage, Aluminium-Verlag, Düsseldorf 2000, 289, 558

[9] Elisental, 10 Juli 2012. [Cited: 10 Juli 2012.] http://www.elisental.de.

[10] F. Ostermann, Anwendungstechnologie Aluminium: 2. neu bearbeitete und aktualisierte Auflage, Springer, Berlin, Heidelberg, New York 2007, 246

[11] Safra, aluminium-copper welding alloys wires & rods, 2012

[12] S. Häuselmann, Magnesium-Halbzeug, 25 Juni 2012, [Cited: 12 Juni 2012.] http://www.haeuselmann.ch.

[13] K. Kerschbaumer et al., (ed.), Das Korrosionsverhalten von MIG-geschweißten Aluminium-Blechen Al5083 und Al6181 im Neutral-Salzsprühnebeltest und die Auswirkung auf die Verbindungsfestigkeit, DVS Congess 2012, Saarbrücken, 2012

[14] EN ISO 9018:2006, Zerstörende Prüfung von Schweißverbindungen an metallischen Werkstoffen – Zugversuch am Doppel-T-Stoß und Überlappstoß, Österreichisches Normungsintitut, Wien 2006

[15] ÖNORM EN ISO 9227, Korrosionsprüfungen in künstlichen Atmosphären – Salzsprühnebelprüfungen, Österreichisches Normungsinstitut, Wien 2006

[16] DIN 8985, Oberflächenprüfung an anschlussfertigen Kühl- und Gefriergeräten, Österreichisches Normungsinsitut, Wien 1983

[17] DIN 50905 Teil 1, Korrosion der Metalle – Korrosionsuntersuchungen-Teil 1, Beuth Verlag GmbH, Berlin 2009, 8

[18] F. Tödt, Korrosion und Korrosionsschutz, 2. Auflage, Walter de Gruyter & Co, Berlin 1961, 143–148, 416–418, 443, 1087

[19] E. Wendler-Kalsch, H. Gräfen, Korrosionsschadenkunde, Springer Verlag, Erlangen 1998, 63, 91–95

[20] K. H. Tostmann, Korrosion – Ursachen und Vermeidung, Wiley – VCH Verlag GmbH, Weinheim 2000, 34, 68–77

[21] G. Schulze, Die Metallurgie des Schweißens, 3., neubearbeitete und erweiterte Auflage, Springer, Berlin 2003, 118, 541

[22] F. Ostermann, Anwendungstechnologie Aluminium: 2. neu bearbeitete Auflage, Meckenheim, Springer, Berlin Deidelberg New York, 2007, 232–248

[23] H. J. Bargel, Werkstoffkunde, 10. bearbeitete Auflage, Springer Verlag, Berlin Heidelberg 2008, 292

[24] C. Kammer, Aluminium Taschenbuch Bd. 1, 16. Auflage, Aluminium Verlag, Düsseldorf 2002, 423

[25] G. E. Totten, D. S. MacKenzie, Handbook of Aluminium, Volume 1, Physical Metallurgy and Processes, Marcel Dekker, Basel 2003, 429

[26] A. Aballe, M. Bethencourt, F. J. Botana, M. J. Cano, M. Marcos, Localized alkaline corrosion of alloy AA5083 in neutral 3.5% NaCl solution, Corrosion Science, 43 (**2001**) 9, 1657–1674

[27] A. Aballe, M. Bethencourt, F. J. Botana, M. Marcos, J. M. Sanchez-Amaya, Influence of the degree of polishing of alloy AA 5083 on its behaviour against localised alkaline corrosion, Corrosion Science, 46 (**2004**) 6, 1909–1920

[28] G. E. Totten, D. S. MacKenzie, Handbook of Aluminium, Volume 2, Alloy Production and Materials Manufacturing, Marcel Dekker Inc., New York, Basel 2003, 435–437

[29] J. R. Davis, Aluminum and aluminium alloys, ASM International, Materials Park, Ohio 1994, Bd. 3., 582

[30] E. Ghali, Corrosion Resistance of Aluminium and Magnesium Alloys, John Wiley & Sons Inc., Hoboken, New Jersey 2010, 171

[31] J. R. Davis et al., ASM Handbook Vol. 2: Poperties and Selection: Nonferrous Alloys and Special-purpose Materials, ASM, USA 2007, 582

[32] W. Hufnagel, Aluminium Taschenbuch, 14. Auflage, Aluminium Verlag, Düsseldorf 1983, 137, 177

[33] R. A. Cottis et al., Shreir's Corrosion forth Edition, Volume 3, Corrosion and degradation of engineering materials, Elsevier, Manchester 2010, 1992, 2025

[34] G. Svenningsen et al., Effect of high temperature heat treatment on intergranular corrosion of AlMgSi(Cu) modell alloy, Corrosion Science, 48 (**2006**), 258–272

[35] G. Svenningsen et al., Effect of low copper content and heat treatment on intergranular corrosion of model AlMgSi alloys, Corrosion Science, 46 (**2006**), 226–242

[36] C. Kammer, Magnesium Taschenbuch; 1. Auflage, Aluminium-Verlag, Düsseldorf 2000, 289

[37] H. Schumann, H. Oettel, Metallografie, 14. Auflage, Wiley-VCH Verlag, Weinheim 2005, 338

[38] K. U. Kainer, Magnesium – Eigenschaften, Anwendungen, Potentiale, Wiley-VCH-Verlag, Weinheim 2000, 238

[39] J. M. Sanchez-Amaya, T. Delgado, L. Gonzalez-Rovira, F. J. Botana, Laser welding of aluminium alloys 5083 and 6082 under conduction regime, Applied Surface Science, 255 (**2009**) 23, 9512-9521

[40] K. Mutombo et al., Corrosion Fatigue Behaviour of Aluminium 5083-H111 Welded Using Gas Metal Arc Welding Method, South Africa, CSIR / University of Pretoria South Africa, 2011

[41] M. Pourbaix, Atlas of Electrochemical Equilibria in Aqueous Solutions, Second English Edition. s.l., Cebelcor Verlag, 1974, 314

[42] H. Göner, S. Marx, Aluminium Handbuch. s.l., VEB Verlag Technik, Berlin 1969

[43] DIN 50905 Teil 2, Korrosion der Metalle-Korrosionsuntersuchungen-Teil 2, Beuth Verlag GmbH, Berlin 1987

[44] DIN 50905 Teil 3, Korrosion der Metalle-Korrosionsuntersuchungen – Teil 3, Beuth Verlag GmbH, Berlin 1987